# AGN and Host Galaxies in the COSMOS Survey

## Christopher D. Impey,[1] Jonathan R. Trump,[2] Jared M. Gabor,[1] and the COSMOS team

[1]Steward Observatory, University of Arizona, 933 North Cherry Avenue, Tucson, AZ 85721

[2]University of California Observatories/Lick Observatory, University of California, Santa Cruz, CA 95064

**Abstract.** The Cosmological Evolution Survey (COSMOS) is a unique tool for studying low level AGN activity and the co-evolution of galaxies and supermassive black holes. COSMOS involves the largest contiguous region of the sky ever imaged by HST; it includes very complete multiwavelength coverage, and the largest joint samples of galaxy and AGN redshifts in any deep survey. The result is a search for AGN with low black hole mass, low accretion rates, and levels of obscuration that can remove them from optical surveys. A complete census of intermediate mass black holes at redshifts of 1 to 3 is required to tell the story of the co-evolution of galaxies and their embedded, and episodically active, black holes.

## 1. Introduction

Until twenty years ago, research on "normal" galaxies and active galactic nuclei was largely decoupled. A small percentage of galaxies displayed nuclear activity that manifested as high excitation and high velocity gas near the nucleus, and the presence of a compact region emitting non-thermal radiation across a wide range of wavelengths (e.g., Seyfert 1943, Schmidt 1961). A paradigm shift occurred when it became clear that all galaxies harbor a supermassive black hole, with a mass scaling according to the population of old stars, and a duty cycle of activity where the nucleus was mostly quiescent (Soltan 1982, Magorrian *et al.* 1998). Alongside that was the realization that active nuclei affect their host galaxies just as profoundly as the immediate environment affects the behavior of the nuclear region (Di Matteo, Springel & Hernquist 2005). The co-evolution of supermassive black holes and galaxies has become a burgeoning research area.

## 2. AGN in the COSMOS Survey

The Cosmological Evolution Survey (COSMOS, Scoville *et al.* 2007) was designed as a survey of galaxy morphology and evolution but the ancillary data that has accumulated around it makes it a peerless resource for studying the demographics and evolution of AGN. The heart of the survey is a 2 deg$^2$, 590-orbit, *i*-band, ACS survey of an equatorial region centered on RA = $10^{\rm h}$, Dec = $+5$ deg (Koekemoer *et al.* 2007). It probes a similar volume for galaxies to the SDSS, but extending fainter and to higher redshift. Multiwavelength data that can be used to select and characterize AGN includes: 1.4 Msec of XMM coverage to a flux of $7 \times 10^{-16}$ cgs, 1.8 Msec of Chandra coverage of the central 1.4 deg$^2$ to a flux of $2 \times 10^{-16}$ cgs, 240 hours of VLA coverage to 10 $\mu$Jy, Spitzer data consisting of 166 hours of IRAC integration complete to 1 $\mu$Jy and 58 hours of MIPS integration to 0.6 mJy, and GALEX coverage to a limit of $m_{\rm AB} \sim 26$. The original

21

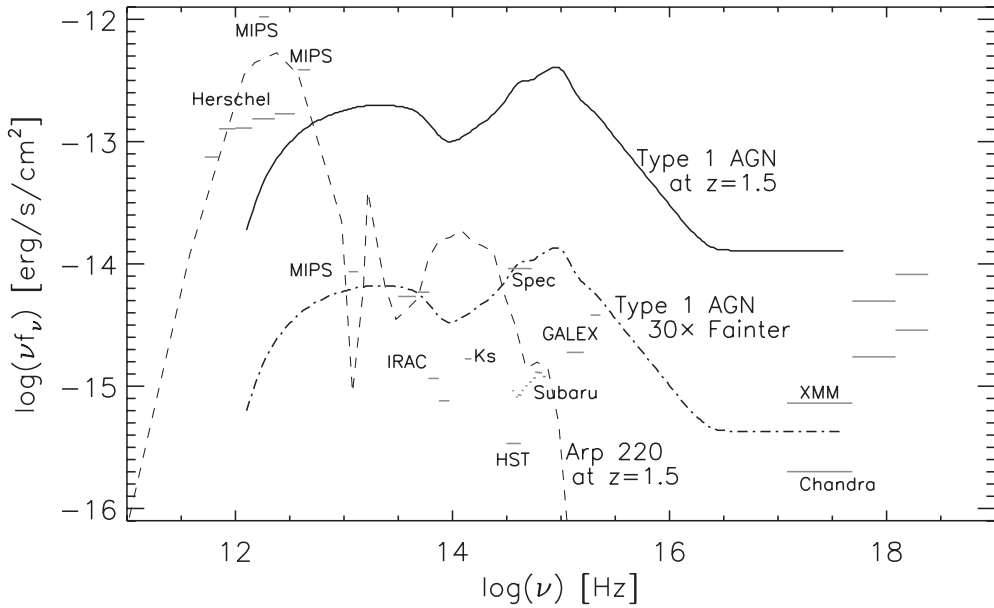**Figure 1.** The $5\sigma$ detection limits across the electromagnetic spectrum for COSMOS are shown as gray lines, and the solid curve is a mean Type 1 SED from Richards *et al.* (2006) at the mean luminosity of the SDSS sample scaled to $z = 1.5$. The dot-dashed line, a factor of thirty lower, represents the luminosity detected by our Magellan/IMACS spectroscopy. The dashed line is the model fit of Silva *et al.* (1998) to Arp 220, a wellstudied local ULIRG and obscured AGN, scaled to z = 1.5. In this energy per unit bandwidth plot, higher regions are the largest contributors to the bolometric luminosity. The Herschel limits represent a GTO program, and all other data has been observed, reduced, and made public.

HST data reached $i_{AB} \sim 26.5$ and it has been augmented by optical and near infrared $uBVgrizJK$ photometry to $m_{AB} = 26$, plus Subaru photometry in 20 intermediate bands (Capak *et al.* 2009). Figure 1 shows the depth of the COSMOS data with respect to a quasar SED and Arp220, both redshifted to $z = 1.5$.

The primary AGN survey using COSMOS (Trump *et al.* 2007, Trump *et al.* 2009a) involves optical identifications of 1465 X-ray sources from a total of 1651 in the XMM survey, of which 677 were targeted for spectroscopy with the IMACS instrument on the Magellan telescope, and 485 of which yielded a secure redshift and identification as an AGN. The limit of the spectroscopic survey was $i_{AB} \sim 23$ and the yield was 288 Type 1 and 149 Type 2 AGN (the remaining 48 AGN were bright in X-rays yet "optically dull" without emission lines, see Trump *et al.* 2009c). The original ACS data was used for studying hosts and environments, and it yielded hosts with Sersic index fits out to $z \sim 1$ and detections out to $z \sim 2$. The completeness of the survey has been tested and calibrated using simulations of mock spectra of varying redshift and optical brightness (Trump *et al.* 2009a). Initial results of the survey are described in the next two sections.

## 3. Black Hole Masses and Accretion Limits

Understanding the role of AGN in galaxy evolution requires measurements of SMBH mass and accretion over the cosmic time. For Type 1 AGN (with broad emission lines), black hole masses can be estimated using single-epoch spectra and virial scaling relations
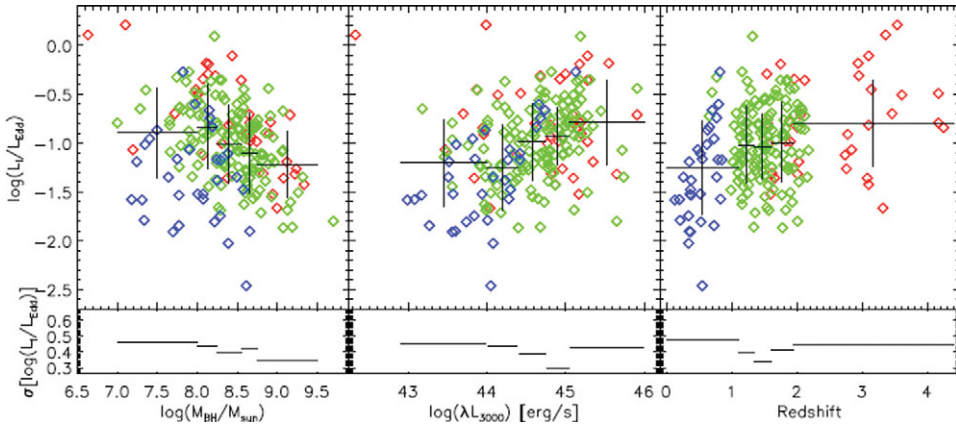
**Figure 2.** The Eddington ratio (accretion rate) with black hole mass, luminosity, and redshift for our Type 1 AGN. Eddington ratio was calculated using an intrinsic luminosity $L_I$ estimated from $L_{3000}$ and $L_{0.5-2\,\mathrm{keV}}$ (Marconi *et al.* 2004). Diamonds represent individual objects with masses estimated from H$\beta$ (blue), Mg II (green), and C IV (red). The large crosses in the top plots show the mean accretion rate in each bin of $M_{BH}$ or redshift, while the gray lines at the bottom show the standard deviation (the square root of the second moment) in each bin. The dispersion deviation is also shown by the vertical error bar in the top plots. Bins were chosen to each have the same number of objects. There are weak trends of $L_I/L_{Edd}$ decreasing with $M_{BH}$ and increasing with $L_{3000}$ and redshift. The dispersion is generally $\gtrsim 0.4$ dex, at least as large as the intrinsic scatter in the $M_{BH}$ scaling relations.

(e.g., Vestergaard & Peterson 2006). These relations estimate black hole mass employ the correlation between the radius of the broad emission line region and the continuum luminosity, $R_{BLR} \sim L^{0.5}$, observed in local AGN with reverberation mapping (Bentz *et al.* 2006). Given the size of the broad line region and its velocity, mass is given by the virial theorem $M_{BH} = f R_{BLR} v_{fwhm}^2$ ($f$ represents the unknown BLR geometry and $v_{fwhm}$ is the velocity width of the broad emission line). In general, masses estimated from the scaling relations are accurate to $\sim 0.4$ dex (Vestergaard *et al.* 2006, Shen *et al.* 2008) and agree with local AGN masses from dynamical estimators (Davies *et al.* 2006, Onken *et al.* 2007) and the $M_{BH}$-$\sigma*$ correlation (Onken *et al.* 2004, Greene *et al.* 2006). Together the mass and the intrinsic accretion luminosity $L_I$ can be used to describe the fueling rate of an AGN in terms of the Eddington ratio, $L_I/L_{Edd}$, where $L_{Edd} = 1.26 \times 10^{38}(M/M_\odot)$ erg s$^{-1}$.

Figure 2 shows the accretion rates with mass, optical luminosity, and redshift for 178 Type 1 AGNs in COSMOS. The size and depth of the COSMOS AGN survey allows for studies spanning 3 decades in mass and luminosity. In contrast with previous work, the depth of COSMOS shows that not all Type 1 AGNs accrete near the Eddington limit, but instead typically have $L_I/L_{Edd} \sim 0.1 \pm 0.5$. However Type 1 AGNs are limited to $L/L_{Edd} > 0.01$, despite simulations which show that the COSMOS AGN detection limits would reveal Type 1 AGNs with $L_I/L_{Edd} \sim 10^{-3}$ (Trump *et al.* 2009b). Optical luminosity and accretion rate are correlated, such that more rapidly accretion AGNs tend to be more optically luminous, (see also Kollmeier *et al.* 2006, Gavignaud *et al.* 2008).

The lack of $L_I/L_{Edd} < 0.01$ Type 1 AGNs and the increase of optical luminosity with accretion rate suggest that accretion rate may cause the transition from Type 1 to Type 2 AGN. As a Type 1 AGN decreases in accretion rate, its optical emission becomes a smaller fraction of its total bolometric output because its cool accretion disk emits less
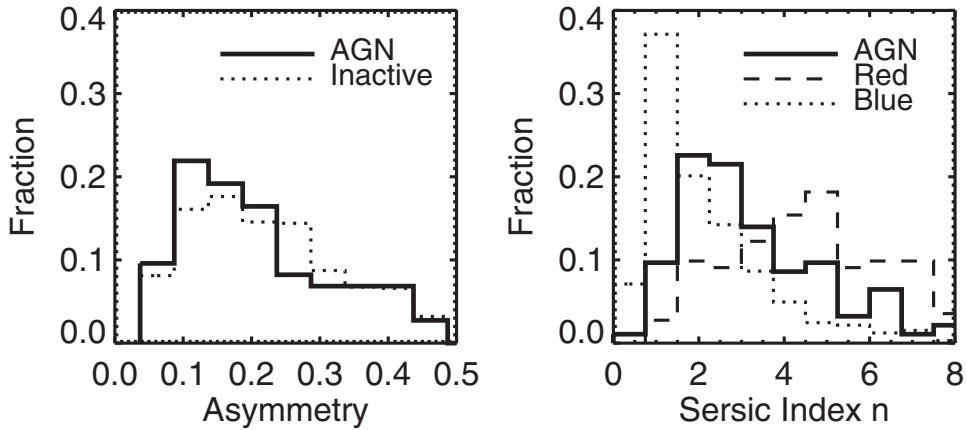
**Figure 3.** Distributions of asymmetry (left panel) and Sersic index (right panel) for AGN hosts and inactive galaxies. AGN hosts are no more *asymmetric* than inactive galaxies, suggesting a fueling mechanism unrelated to mergers. At right, inactive galaxies are split into blue star–forming and red quiescent galaxies. AGN hosts are more likely to be bulge-dominated than the typical normal galaxy, yet a significant fraction ($\sim 40\%$) are disk-dominated (Gabor *et al.* 2009).

brightly. Thus a more rapidly accreting Type 1 AGN has more emission from its cool (optical) disk than its hot (X-ray) corona, consistent with the results of Kelly *et al.* (2008), which show that $\alpha_{OX}$ (the ratio between optical/UV and X-ray flux) becomes more X-ray quiet with accretion rate, possibly because the disk grows larger or thicker as the accretion rate approaches the Eddington limit. At accretion rates below $L_I/L_{Edd} \sim 0.01$, the optical disk changes so much that the broad line region is no longer supported, and broad emission lines are not observed in the spectrum. AGNs with $L_I/L_{Edd} < 0.01$ are probably observed instead as unobscured Type 2 AGNs (Trump *et al.* 2011).

## 4. Host Galaxies and Environments

Simulations suggest that gas-rich major mergers are an efficient mechanism for triggering AGN (e.g., Hernquist 1989, Hopkins *et al.* 2005). Taken at face value, this result implies that galaxies hosting AGN should be morphologically disturbed. Furthermore, since major mergers tend to turn stellar disks into spheroids (Barnes 1990), we expect AGN host galaxies to be spheroid-dominated. Using the centerpiece $F814W$ ACS images of COSMOS, we can reliably measure AGN host galaxy morphologies out to $z \sim 1$. Measurements of asymmetric morphologies indicate recent galaxy mergers that may have induced black hole fueling (Conselice *et al.* 2000), and measurements of the Sersic index indicate whether a galaxy is disk-dominated ($n = 1$) or spheroid-dominated ($n = 4$).

The sheer size of the COSMOS field enables the construction of large ($\times 10$) control samples of inactive galaxies. We match AGN host galaxies to normal galaxies in $I$-band absolute magnitude and redshift, and compare their morphological properties. For the AGN sample, we carefully account for any bright point source by fitting a PSF component simultaneously with the galaxy component using GALFIT (Peng *et al.* 2002). By subtracting the PSF component we measure asymmetries in the light distribution in an unbiased way, but our measurements are far more reliable for narrow-line, "obscured" AGN than for those with broad lines (Gabor *et al.* 2009).

We find little evidence that major mergers trigger AGN fueling, at least for moderate-luminosity ($10^{42-44}$ erg s$^{-1}$) X-ray- selected samples without broad optical emission lines (Gabor *et al.* 2009). Figure 3 shows that AGN host galaxy morphologies are no more asymmetric than those of a control sample. Interestingly, AGN host galaxies are not simply bulge-dominated ($n > 2.5$) systems, but show a broad range of morpohologies. A substantial fraction ($\sim$40 %) of our AGNs reside in disk-dominated galaxies, and this remains true when accounting for substantial systematic uncertainties. The AGN sample is not just a random sampling of normal galaxies, however – AGN hosts are more likely to be bulge-dominated than the average inactive galaxy. These results, which are borne out with "by-eye" morphological classification (Cisternas *et al.* 2011), indicate that mergers are not required for AGN fueling.

## References

Barnes, J. E. 1980, Nature, 344, 379

Bentz, M. C., Peterson, B. M., Pogge, R. W., Vestergaard, M., & Onken, 2006, C. A. *ApJ*, 644, 133

Capak, P. *et al.* 2010, *in prep.*

Cisternas, M., *et al.* 2011, ApJ, 726, 57

Conselice, C. J., Bershady, M. A., & Jangren, A. 2000, ApJ, 529, 886

Davies, R. I., *et al.* 2006, *ApJ*, 646, 754

Di Matteo, T., Springel, V., & Hernquist, L. 2005, Nature, 433, 604

Gabor, J. M., *et al.* 2009, ApJ, 691, 705

Gavignaud, I., *et al.* 2008, *A&A*, 492, 637

Greene, J. E. & Ho, L. C. 2006, *ApJ*, 641, 21

Hernquist, L. 1989, Nature, 340, 687

Hopkins, P. F., Hernquist, L., Cox, T. J., & Di Matteo, T. 2005, *ApJ*, 630, 705

Koekemoer, A. M., *et al.* 2007, *ApJS*, 172, 196

Kollmeier, J. A., *et al.* 2006, *ApJ*, 648, 128

Magorrian, J., *et al.* 1998, *AJ*, 115, 2285

Marconi, A., Risaliti, G., Gilli, R., Hunt, L. K., Maiolino, R., & Salvati, M. 2004, *MNRAS*, 351, 169

Onken, C. A., Ferrarese, L., Merritt, D., Peterson, B. M., Pogge, R. W., Vestergaard, M., & Wandel, A. 2004, *ApJ*, 615, 645

Onken, C. A., *et al.* 2007, *ApJ*, 670, 105

Peng, C. Y., Ho, L. C., Impey, C. D., & Rix, H.-W. 2002, *AJ*, 124, 266

Schmidt, M. 1963, Nature, 197, 1040

Scoville, N., *et al.* 2007, *ApJS*, 172, 38

Seyfert, C. K. 1943, ApJ, 97, 28

Shen, Y., Greene, J. E., Strauss, M. A., Richards, G. T., & Schneider, D. P. 2008, *ApJ*, 680, 169

Soltan, A. 1982, MNRAS, 200, 115

Trump, J. R., *et al.* 2007, *ApJS*, 172, 383

Trump, J. R., *et al.* 2009a, *ApJ*, 696, 1195

Trump, J. R., *et al.* 2009b, *ApJ*, 700, 49

Trump, J. R., *et al.* 2009c, *ApJ*, 706, 797

Trump, J. R., *et al.* 2011, *ApJ* submitted

Vestergaard, M. & Peterson, B. M. 2006, *ApJ*, 641, 689